RESEARCH PAPER
*Contrib. Sci. & Tech Eng, 2025, 2(2)*
*Homepage: https://cste.journals.umz.ac.ir/*
*DOI: 10.22080/cste.2025.28773.1018*

# Numerical Investigation of the Effect of Scale, Loading Rate, and Lateral Load on the Stress-Strain Behavior of Rock Under Pressure

**Majid Noorian-Bidgoli [1]*, Mahboobeh Koochaki [2]**

[1] *Associate Professor, Department of Mining Engineering, Faculty of Engineering, University of Kashan, Kashan, Iran.*

[2] *Master Student, Department of Mining Engineering, Faculty of Engineering, University of Kashan, Kashan, Iran*

**Article Info**
Received 07 March 2025
Accepted 08 May 2025
Available online 12 June 2025

**Keywords:**
Compressive Strength;
Stress-Strain Behavior;
Rock;
Numerical Modeling;
Finite Difference Method (FDM).

**Abstract:**
In this study, uniaxial and biaxial compression tests were simulated to assess the impact of sample scale, both dimensions and shape, along with the rate and nature of loading on the strength behavior and deformability of a limestone rock specimen. For this end, the finite difference method (FDM) using FLAC code was employed. The compression test simulations utilized an innovative technique based on the model's equilibrium principle during loading, mimicking static loading conditions in reality. This approach facilitated systematic control of axial and lateral loads on the model, effectively preventing abrupt, violent failure. A series of two-dimensional (2D) models was subjected to varying loading conditions to appraise the stress-strain behavior of the computational models. Numerical results show that changes in the model's shape and dimensions affected the compressive strength of rock models. Here, an increment in the width-to-length ratio of the model led to enhanced compressive strength. Similarly, an increase in the loading rate also increased the uniaxial compressive strength of the model. Also, the rock model's compressive strength was further increased by applying and augmenting lateral pressure in the biaxial compression test. Hence, rocks under pressure demonstrate scale-dependent behaviors, exhibiting varying strengths under different loading conditions.



***Corresponding Author:** noriyan@kashanu.ac.ir

**Supplementary information:** Supplementary information for this article is available at https://cste.journals.umz.ac.ir/

**Please cite this paper as:** Noorian-Bidgoli, M. , & Koochaki, M. (2025). Numerical investigation of the effect of scale, loading rate, and lateral load on the stress-strain behavior of rock under pressure. Contributions of Science and Technology for Engineering, 2(2), 47-55. doi:10.22080/cste.2025.28773.1018.

## 1. Introduction

Assessing the mechanical behavior of rocks and determining the mechanism and failure criterion necessitates understanding strength parameters, such as the uniaxial and biaxial compressive strength of rock masses. These parameters are integral to the design and stability analysis of various surface and subsurface structures, including rock slopes of surface mine faces, trenches, dams, roads, and excavations of underground mines, tunnels, shafts, and caves. Furthermore, these parameters are crucial in deciding the different stages of mining unit operations, namely drilling, blasting, digging, and cutting, and all types of support systems for surface and underground structures in civil and mining engineering [1, 2].

Given the heterogeneity and anisotropy of rocks, the strength and deformability parameters of each rock type must be measured precisely, considering the initial and boundary conditions of the area. Presently, direct methods, such as in-site and laboratory tests, and indirect tests, such as employing theoretical-experimental relationships and numerical-analytical methods, offer a variety of solutions for determining the compressive strength of rocks [3].

Direct methods, such as field tests, can prove to be costly and time-consuming due to operational challenges. Furthermore, laboratory techniques are limited by their ability to apply only some natural conditions of the area. Nevertheless, standard laboratory procedures for measuring compressive strength have been provided by entities such as the American Society for Testing and Materials (ASTM) and the International Society of Rock Mechanics (ISRM) [4]. While these techniques are relatively straightforward, they tend to be both time-consuming and expensive, requiring meticulous preparation of rock specimens. For carbonate rocks like limestone, this process often poses a challenge [5].

When initiating engineering projects, the strength parameters of rocks can be determined quickly and at a low cost using indirect tests such as point load index [6-12], Schmidt hammer [13-19], sound speed [20-23], cyclic



*ISSN **3060-6578***

loading [24], and even small-scale experiments [25]. Laboratory studies, for instance, have shown that the uniaxial compressive strength of limestone directly correlates with the rock's density [26], while it inversely correlates with environmental humidity [27-29]. However, the precision of these methods tends to be insufficient in practical scenarios, frequently necessitating the use of alternative approaches.

To establish the strength parameters of rocks, researchers have proposed experimental and theoretical criteria based on data gathered and experiences drawn from various projects. These include the Mohr-Coulumb [30], Baniawski [31], Johnston [32], Ramamurthy et al. [33], and Hoek and Brown [34] strength criteria. A significant drawback of these relationships is their specificity to certain areas, aligning with the conditions of the experimental criterion. Consequently, their applicability is not universal.

Over the past decades, the advent of advanced computing equipment has led to the development of several analytical methods based on operations research. These include techniques like the adaptive neuro-fuzzy inference system (ANFIS), artificial neural network (ANN), Monte-Carlo simulation, meta-heuristic and evolutionary algorithms, and linear and non-linear regression. These methods have been used to determine the rock strength parameters [35-39]. Despite their high flexibility, reduced calculation time, and ability to use both quantitative and qualitative criteria simultaneously, these methods are often associated with high uncertainty due to their random basis.

Among analytical techniques, numerical methods offer unique capabilities for creating both continuous and discontinuous models, encompassing rock and discontinuity. These methods allow the rock to be divided into numerous small elements, facilitating a detailed, accurate, and rapid examination of each element's mechanical behavior and interdependencies [40]. Past studies have demonstrated these methods' capacity to accurately determine the strength parameters of various types of rock and rock mass under static and dynamic loading conditions [41-50]. Consequently, by simulating direct and indirect tests using these methods, the rock's strength behavior and deformability can be estimated accurately, quickly, and cost-effectively, while maintaining conditions similar to those in nature.

The most common method for studying rock mechanical behavior involves applying axial compression to a circular cylinder sample two to three times longer than its diameter. When the rock's lateral surface is free from traction, this setup is called uniaxial or unconfined compression. The results can be represented in a stress-strain curve, with stress (σ) plotted against strain (ε) (Figure 1). Based on this figure, behavior within the range of stress and strain before failure is known as linearly elastic. The stress value at point B, which indicates the transition from elastic to ductile behavior, is referred to as the yield stress of the rock. Also, the stress value at point C, which indicates the transition from ductile to brittle behavior, is referred to as the uniaxial compressive strength (UCS) of the rock. In the ductile regime, corresponding to region BC of this figure, the transverse strains increase in magnitude much more rapidly than the axial strain. The failure process is ongoing throughout the brittle region designated as CE. The rock physically deteriorates during this process, decreasing its ability to support a load. Thus, failure begins at point C. For a rock subjected to uniaxial compression, the criteria for failure can be defined simply as the condition under which failure occurs [30, 51].

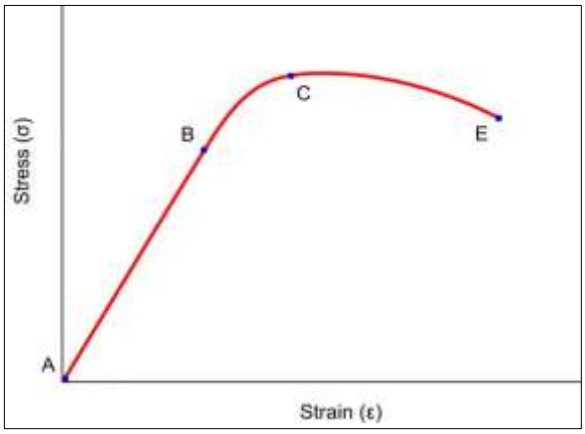


**Figure 1. Complete stress-strain curve for a rock sample under compression**

In this study, the finite difference method (FDM) has been used for numerical modeling, with a focus on examining the influence of scale, rate, and type of loading on the mechanical behavior of rocks under pressure. Standard uniaxial and biaxial compression tests were simulated in FLAC2D software, investigating the mechanical behavior of a limestone sample through stress-strain curves. In this context, while establishing the strength behavior of the samples under pressure, the impact of the aforementioned external factors on the compressive strength of the model was determined at each stage.

## 2. Modeling of Compressive Strength Test

The finite difference method is a numerical method rooted in differential equations, suitable for modeling continuous media with non-linear behavior. In this method, each derivative of the governing equations is directly defined by an algebraic description in terms of model variables (such as stress or displacement) at distinct points of the model geometry. Initially, motion equations were utilized to derive new velocities and displacements resulting from the application of stresses and forces. Subsequently, strain rates were calculated from the velocity values, and the new stress values were obtained from the new strain rates. Each computational cycle occurs in one step. If the time steps of computation are sufficiently small, the results obtained in one region over a short time span will not impact neighboring regions. Thus, after several steps in the analysis, environmental changes are applied across all model elements.

FLAC, featuring fast Lagrangian analysis capability, is a powerful software based on the finite difference numerical method, using an explicit time-dependent approach to

solve algebraic equations [34]. The general analysis method in this software involves dividing the model's geometry into smaller elements with identical numerical characteristics, followed by solving the differential equation associated with each element until the relative equilibrium of the model is achieved. Owing to the software's high flexibility in modeling and analyzing problems, its usage has broadened to predict the strength behavior and deformability of various materials, such as soil or rock, under different loading conditions. Hence, this research employed software to model compression tests on rock using a novel technique - the equilibrium of model points at each step. This research's novelty lies in its extension of the mathematical platform established by Noorian-Bidgoli et al. [45] for a DFM model to study the stress-strain behavior of rock under pressure.

## 2.1. Geometry and Meshing of the Model

The two-dimensional version of the numerical code, FLAC2D, is utilized for simulation under plane strain conditions [52]. In this instance, a two-dimensional geometric model of the problem is constructed, allowing the removal of one of the strain components along the x, y, and z axes. Given the aim of this research to model rock compressive tests, the model's geometry is fashioned in accordance with standard laboratory tests, that is, a cylindrical sample under loading.

In this research, six scale types were employed to construct the model's geometry to examine the effect of scale (length and width of the sample) on the rock sample's compressive strength, as per Table 1. Typically, the length of the sample (L) in a standard rock compressive test (ISRM standard) is considered to be between 1.50 and 2.50 times the diameter or width of the sample (D). As NX is chosen for the rock samples in the laboratory, the base width of the model is selected as 54 mm. Consequently, the model's length in the first case is chosen as 1.50, 2.50, and 3.50 times the width. In the second case, these values are reversed. Non-standard values were chosen to conduct a sensitivity analysis of the sample scale, as it is an important variable in determining rock compressive strength. These dimensional ranges are used to investigate the effect of the sample scale on the stress-strain behavior of rock under pressure.

**Table 1. Dimensions of the numerical models**

| Model number | Length or L (cm) | Width or D (cm) | Length to width ratio (L/D) |
|---|---|---|---|
| 1 | 8.10 | 5.40 | 1.50 |
| 2 | 13.50 | 5.40 | 2.50 |
| 3 | 18.90 | 5.40 | 3.50 |
| 4 | 5.40 | 8.10 | 0.67 |
| 5 | 5.40 | 13.50 | 0.40 |
| 6 | 5.40 | 18.90 | 0.29 |

Notably, all the mentioned models assume intact rock without discontinuities. In the following stage, models are meshed with square meshes (10×20), mirroring the shape of the rock sample (Figure 2). Each model element contains four nodes, meaning that the derivatives in the problem's governing differential equation replace their approximate values at the node.

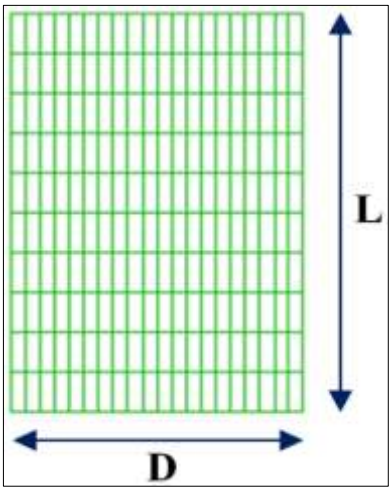


**Figure 2. Geometry and meshing of the numerical model**

## 2.2. Behavior and Mechanical Properties of the Model

The Mohr-Coulomb behavioral model was employed in this research to investigate the stress-strain behavior of rocks under compressive loading. This model is used because it is the closest one to simulating limestone behavior among a few material models supported by the FLAC2D software. Additionally, the necessary data for utilizing this model were available in this study. This failure criterion characterizes the behavior of materials based on the shear failure equation and ultimate tensile strength. The availability of necessary information for modeling informed this choice. This behavior model, based on principal stress values, is offered in FLAC software, effectively representing the principal stress vector in the Mohr-Coulomb criterion. The mechanical properties of limestone used in modeling are presented in Table 2.

**Table 2. Mechanical properties of the numerical models**

| Parameter | Unit | Value |
|---|---|---|
| Density | $Kg/m^3$ | 2700 |
| Modulus of elasticity | GPa | 96 |
| Poisson's ratio | - | 0.37 |
| Cohesion | MPa | 9.17 |
| Friction angle | ◦ | 25.68 |

## 2.3. Boundary and Initial Conditions of the Model

To model the compressive tests (uniaxial and biaxial) akin to laboratory loading conditions, a compressive load along the vertical axis (y) was applied to the model's upper surface. This loading was uniformly and continuously conducted during the model execution. In this context, a lower loading rate requires more modeling time but yields more accurate results. Therefore, a loading rate of 0.001 m/s was selected for this research to enhance the accuracy

of calculations. Furthermore, to mitigate fluctuations caused by the model's sudden failure during loading, the local damping ability of static loading was utilized on the model.

As shown in Figure 3-a, in the uniaxial rock compressive test modeling, the model's two side walls (right and left) are defined without loading and left free. Additionally, by setting the boundary of the model at the model's bottom level (floor), displacement is considered zero in both horizontal and vertical directions. In Figure 3, y signifies the initial axial compressive load on the model's upper surface, while Δy denotes the loading rate at each loading step. Consequently, y+Δy represents the sum of the initial and increased axial load at the conclusion of each loading step on the model.

According to Figure 3-b, in the biaxial compressive test modeling, an additional constant compressive load in the horizontal axial direction (x) is applied to the model's lateral surfaces in conjunction with the axial load seen in the uniaxial compressive test. Essentially, the model's lateral pressures or confining pressures align with the horizontal stresses in the ground or the hydraulic pressure of the fluid in the laboratory, which can be factored into the modeling. In this research, six values of lateral load have been employed to investigate the impact of lateral pressure on mechanical behavior and the final strength of the rock, as per Table 3.

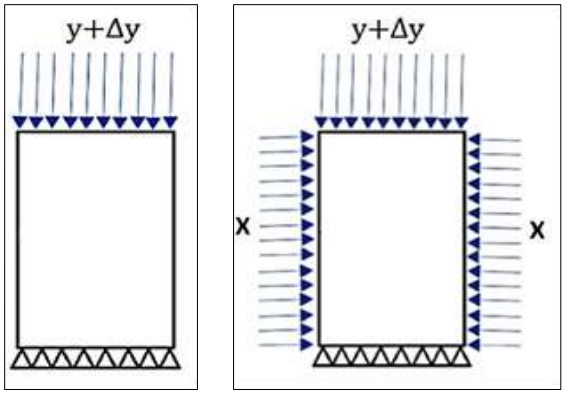


**Figure 3. Boundary conditions of the model in (a) Uniaxial and (b) Biaxial compressive strength test**

**Table 3. Lateral loading values to model of the biaxial compressive strength test**

| Loading type | Lateral loading rate (m/s) |
|---|---|
| 1 | 0.01 |
| 2 | 0.03 |
| 3 | 0.05 |
| 4 | 0.07 |
| 5 | 0.09 |
| 6 | 0.10 |

## 2.4. Running of the model

In FLAC, model execution and loading cycle application can either be performed manually or automatically. The automatic method, typically executed by defining a loop in the model, is faster but less precise. In this case, without inspecting the equilibrium of all the model points during the loading time, the model is saved after each execution, and the next step commences. As a result, it is impossible to verify the equilibrium of all model points after each loading step. Most research in the literature applies automatic loading to the model, which can compromise accuracy.

For this research, a model has been developed using Fish programming via an innovative technique to enhance calculation accuracy. In this method, the model is manually run in each loading cycle, and the history of unbalanced forces at the observation points is scrutinized to ensure the model reaches equilibrium at the end of each execution step. In this context, if the model has not achieved equilibrium, the loading cycle is extended. Concurrently, the condition of the unbalanced forces of the observation points is regularly checked until the model achieves equilibrium. Therefore, in this method, the current loading cycle is saved when the model reaches equilibrium. The model is then reloaded at the beginning of the next loading cycle. This process continues until the modeled rock sample fails.

In the code, the history command enables recording various parameter changes during model execution at pre-defined points (observation points). Hence, changes such as displacement, stress, strain, and so on, at the observation points are recorded at variable time intervals. For this research, nine observation points have been defined for each model, with the location of these points remaining fixed across all models. These points include four points at the four corners of the model (two upper and two lower corners), two points at the center of the model's upper and lower surfaces, two points in the centers of the lateral surfaces, and one point at the model's center of gravity.

Figure 4 schematically presents the location of the aforementioned observation points on one of the models. The model's equilibrium is monitored and controlled using these points during loading. For instance, the changes in unbalanced forces over time during the execution of one of the models in the initial ten loading steps of the uniaxial compressive strength test are depicted in Figure 5. This figure indicates that the quantity of unbalanced forces reaches zero or near zero at each loading, signifying the model's equilibrium at the completed steps, ten steps in this figure.

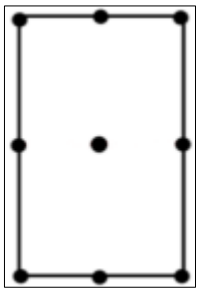

**Figure 4. Schematic of the location of 9 observation points on the model**

## 3. Results and Discussion

Simulations were conducted under uniaxial and biaxial loading conditions until the peak strength of the tested model was achieved. After each modeling, axial stress versus axial strain curves (stress-strain curves) were plotted to assess the mechanical behavior of the rock models.

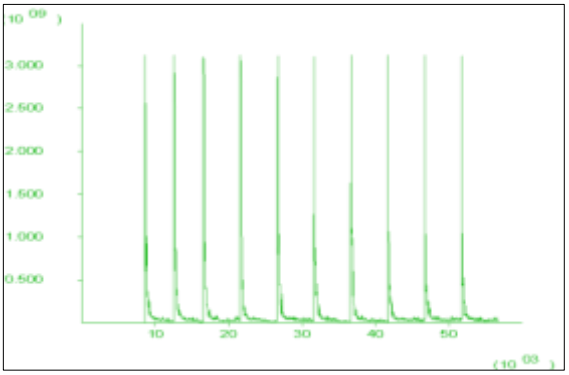

**Figure 5. Variations of unbalanced forces with respect to time during the uniaxial compressive strength test**

### 3.1. Effect of Sample Scale

As previously explained, to examine the effect of sample sizes (changes in length and width) on the mechanical behavior of rock models under pressure, six models were constructed according to Table 1, with uniaxial compression tests performed on all of them. Ultimately, results were derived in the form of stress-strain curves (Figure 6). The number of execution cycles until the final solution for each model for samples with D/L ratios of 1.50, 2.50, and 3.50 was 51569, 55695, and 56646, respectively. For samples with L/D ratios of 1.50, 2.50, and 3.50, these figures were 41569, 47659, and 52428, respectively.

As observable in Figure 6, the value of peak uniaxial compressive strength (marked points under each sample) decreases with the increase in length (L) and the length-to-width ratio (L/D) of the model. On the other hand, the rock sample's strength increases as the width-to-length ratio increases. The reasons for these trends differ from those observed in cases purely related to size. When a model is subjected to uniaxial compression, loading end platens, preferably the same diameter as the model, are employed. Due to an unavoidable mismatch in the elastic properties of the rock and the platens, a complex zone of triaxial compression forms at the ends of the rock model as the platen restricts the rock's expansion. Therefore, this end effect is not significant for a slender model but can dominate the stress field in a squat model.

This outcome can also be attributed to the reduced likelihood of failure due to bending with shorter sample lengths, enabling the model to reach its ultimate strength over more cycles. Furthermore, this figure shows that with the increase of width (D) and the model's width-to-length ratio (D/L), the peak uniaxial compressive strength value escalates. The reasoning behind this observation could be that an increased model width reduces the amount of force per unit area (pressure), delaying sample fractures and thereby boosting strength.

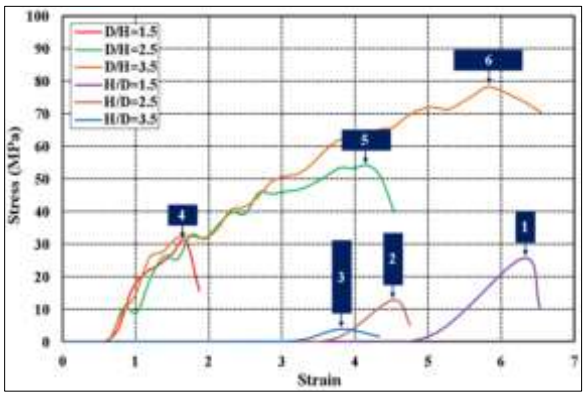


**Figure 6. The effect of sample scale on the mechanical behavior of the rock model**

Moreover, comparing the deformation behavior of the models reveals that when the model's length surpasses its width (models No. 1, 2, and 3), the fracture behavior mimics that of brittle rocks. Conversely, ductile fracture behavior is observed when the model's width is larger than its length (models no. 4, 5, and 6). Therefore, the ductility increases as the ratio of width to length of the rock sample increases. Prior experimental results have exhibited similar behaviors [53], indicating that reducing the sample's diameter-to-length ratio shifts the rock's mechanical behavior under pressure from ductile to brittle.

### 3.2. Effect of Loading Rate

This section presents the results of uniaxial compressive test modeling on a standard sample with a length-to-width ratio (L/D) of 2.50, aiming to investigate the effect of the loading rate. Three loading rate values of 0.001, 0.003, and 0.005 have been employed under the same conditions illustrated in Figure 3-a.

Figure 7 depicts the results derived from the three types of loading in the form of stress-strain curves. As evident, the uniaxial compressive strength significantly increases with the escalation of the loading rate on the model under pressure. Notably, the mechanical behavior of the model remains consistent in all three loading rate conditions, with all models exhibiting entirely brittle stress-strain behavior.

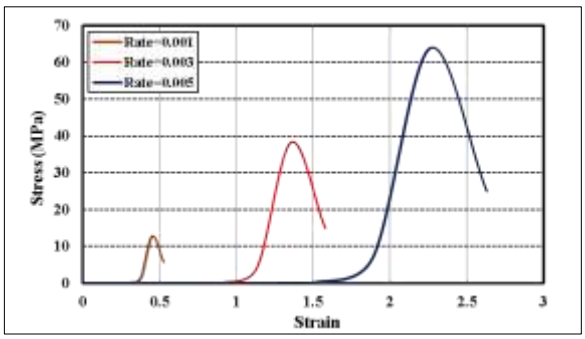


**Figure 7. The effect of loading rate on the mechanical behavior of the rock model**

Commonly in practice, the loading rate in compression tests is applied as the stress or strain rate of change per time unit on rock samples. For instance, most automatic testing devices (servo-control) for uniaxial compressive strength tests usually apply strain or displacement control loading. Herein, based on the sample sizes and strain rate, the loading rate can be selected and applied to the rock models. The total form of the stress-strain curve is a function of the applied strain rate. A lower strain rate leads to a decrease in compressive strength.

Prior laboratory studies on various rock samples have indicated that an increased loading speed augments uniaxial compressive strength [54]. Thus, in the laboratory, testing hard rocks at higher loading speeds is typically preferred, while softer rocks are tested at lower loading speeds. Consequently, adherence to laboratory standards and the correct selection of the loading rate can play a vital role in successfully determining the compressive strength and mechanical behavior of rocks.

### 3.3. Effect of Confining Load

A biaxial compression test has been modeled to examine the effect of lateral or confining load on the model's mechanical behavior. The behavior of the models under six different types of lateral loads, akin to the values in Table 3, is presented in Figure 8 in the form of stress-strain curves. As depicted in this figure, the rise in confining pressure enhances the compressive strength of the rock model under biaxial pressure. This can be attributed to the prevention of deformation or high lateral strains through the application and increase of confining pressure, delaying the sample's yielding and failure limit and, in turn, escalating the strength. Additionally, this figure implies that with the growth of confining pressure, the model's behavior transitions from brittle to ductile, a phenomenon also observed in previous practical studies by Mogi [55]. The stress-strain curve initially shows a nearly linear elastic segment, with a slope (Young's modulus) that is mostly unaffected by the confining stress.

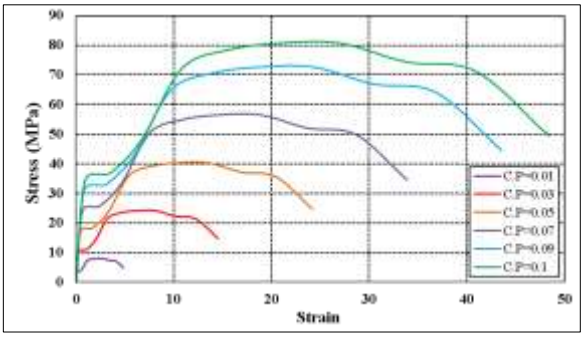


**Figure 8. The effect of confining load on the mechanical behavior of the rock model**

## 4. Conclusions

External factors such as scale, loading rate, and confining load significantly influence the mechanical behavior of rocks under pressure, necessitating their consideration when determining the strength behavior and deformability of rocks. These elements, independent of the rock's inherent characteristics, depend on the experimental conditions and can be controlled. Thus, the effects of these factors must be correctly determined to achieve accurate results. This research developed a systematic 2D numerical procedure using the FLAC finite difference code to examine the stress-strain behavior of a limestone sample under uniaxial and biaxial compressive loading. Key conclusions from this research can be summarized as follows:

- An increase in the sample's width (diameter) to length (height) ratio elevates the sample's compressive strength under uniaxial pressure and vice versa. This size enlargement alters the model's mechanical behavior from brittle to ductile. This outcome underscores the importance of sample size and shape in rock testing, as it could yield different results due to variations in the applied load on the surface.

- A higher loading rate on the pressure-subjected sample enhances its uniaxial compressive strength. In this context, the model's mechanical behavior remains consistent across various loading rates, with all models exhibiting entirely brittle stress-strain behavior. Consequently, the stress-strain behavior of rocks significantly depends on the loading rate.

- Confining load application on an axially loaded specimen amplifies its compressive strength compared to the unconfined state. Increased confining load and strength enhancement shift the rock model's stress-strain behavior from brittle to ductile. These findings hold considerable implications for investigations into rock strength under pressure.

Overall, it is concluded that the external factors studied in this research influenced the results of simulated pressure tests significantly. The modeled rock samples exhibit robust scale-dependent stress-strain behaviors with varying strengths under different loading conditions. Therefore, rock tests must adhere to the guidelines of common standards; otherwise, the results could substantially deviate. In this context, numerical modeling emerges as a potent tool that can accurately determine these factors' effects on fracture behavior and types of rock strength, obviating the need for time-consuming and costly practical tests. Sensitivity analysis using these methods can mitigate the risk of potential misestimation of rock strength and deformability parameters.

Utilizing the models developed in this research allows the exploration of the effects of internal or intrinsic factors on rock mechanical behavior. The authors are currently investigating this topic and anticipate future publications.

## 5. References

[1] Bieniawski, Z. T. (1974). Geomechanics Classification of Rock Masses and Its Application in Tunneling. Proceedings of 3rd Congress of the International Society of Rock Mechanics, Denever National Academy of Sciences, Denver, United States.

[2] Cargill, J. S., & Shakoor, A. (1990). Evaluation of empirical methods for measuring the uniaxial compressive strength of rock. International Journal of Rock Mechanics and Mining Sciences & Geomechanics Abstracts, 27(6), 495–503. doi:10.1016/0148-9062(90)91001-N.

[3] Kanji, M., He, M., & Ribeiro e Sousa, L. (Eds.). (2020). Soft Rock Mechanics and Engineering. Springer, Cham, Switzerland. doi:10.1007/978-3-030-29477-9.

[4] Ulusay, R. (Ed.). (2015). The ISRM Suggested Methods for Rock Characterization, Testing and Monitoring: 2007-2014. Springer, Cham, Switzerland. doi:10.1007/978-3-319-07713-0.

[5] Zhang, L. (2016). Engineering properties of rocks. Butterworth-Heinemann, Waltham, United States.

[6] Hawkins, A. B., & Oivert, J. A. G. (1986). Point Load Tests: Correlation factors and contractual use. An example from the Corallian at Weymouth. Geological Society Engineering Geology Special Publication, 2(1), 269–271. doi:10.1144/GSL.1986.002.01.48.

[7] Romana, M. (1999). Correlation between uniaxial compressive and point-load (Franklin test) strengths for different rock classes. 9th ISRM Congress, 25 August, 1999 Paris, France.

[8] Rusnak, J., & Mark, C. (2000). Using the point load test to determine the uniaxial compressive strength of coal measure rock. Proceedings of the 19th International Conference on Ground Control in Mining, August 8-10, 2000, Morgantown, United States.

[9] Tsiambaos, G., & Sabatakakis, N. (2004). Considerations on strength of intact sedimentary rocks. Engineering Geology, 72(3–4), 261–273. doi:10.1016/j.enggeo.2003.10.001.

[10] Singh, T. N., Kainthola, A., & Venkatesh, A. (2012). Correlation between point load index and uniaxial compressive strength for different rock types. Rock Mechanics and Rock Engineering, 45(2), 259–264. doi:10.1007/s00603-011-0192-z.

[11] Garrido, M. E., Petnga, F. B., Martínez-Ibáñez, V., Serón, J. B., Hidalgo-Signes, C., & Tomás, R. (2022). Predicting the Uniaxial Compressive Strength of a Limestone Exposed to High Temperatures by Point Load and Leeb Rebound Hardness Testing. Rock Mechanics and Rock Engineering, 55(1), 1–17. doi:10.1007/s00603-021-02647-0.

[12] Sadeghi, E., Nikudel, M. R., Khamehchiyan, M., & Kavussi, A. (2022). Estimation of Unconfined Compressive Strength (UCS) of Carbonate Rocks by Index Mechanical Tests and Specimen Size Properties: Central Alborz Zone of Iran. Rock Mechanics and Rock Engineering, 55(1), 125–145. doi:10.1007/s00603-021-02532-w.

[13] Sachpazis, C. I. (1990). Correlating schmidt hardness with compressive strength and young's modulus of carbonate rocks. Bulletin of the International Association of Engineering Geology, 42(1), 75–83. doi:10.1007/BF02592622.

[14] Katz, O., Reches, Z., & Roegiers, J. C. (2000). Evaluation of mechanical rock properties using a Schmidt Hammer. International Journal of Rock Mechanics and Mining Sciences, 37(4), 723–728. doi:10.1016/S1365-1609(00)00004-6.

[15] Kahraman, S. (2001). Evaluation of simple methods for assessing the uniaxial compressive strength of rock. International Journal of Rock Mechanics and Mining Sciences, 38(7), 981–994. doi:10.1016/S1365-1609(01)00039-9.

[16] Mostyn, G. R., & Li, K. S. (2020). Probabilistic slope analysis — State-of-play. Probabilistic Methods in Geotechnical Engineering, 89–109. doi:10.1201/9781003077749-6.

[17] Yaşar, E., & Erdoğan, Y. (2004). Estimation of rock physicomechanical properties using hardness methods. Engineering Geology, 71(3–4), 281–288. doi:10.1016/S0013-7952(03)00141-8.

[18] Shalabi, F. I., Cording, E. J., & Al-Hattamleh, O. H. (2007). Estimation of rock engineering properties using hardness tests. Engineering Geology, 90(3–4), 138–147. doi:10.1016/j.enggeo.2006.12.006.

[19] Aldeeky, H., Al Hattamleh, O., & Rababah, S. (2020). Assessing the uniaxial compressive strength and tangent Young's modulus of basalt rock using the leeb rebound hardness test. Materiales de Construccion, 70(340), 230–230. doi:10.3989/MC.2020.15119.

[20] Pappalardo, G. (2015). Correlation Between P-Wave Velocity and Physical–Mechanical Properties of Intensely Jointed Dolostones, Peloritani Mounts, NE Sicily. Rock Mechanics and Rock Engineering, 48(4), 1711–1721. doi:10.1007/s00603-014-0607-8.

[21] Abdelhedi, M., Aloui, M., Mnif, T., & Abbes, C. (2017). Ultrasonic velocity as a tool for mechanical and physical parameters prediction within carbonate rocks. Geomechanics and Engineering, 13(3), 371–384. doi:10.12989/gae.2017.13.3.371.

[22] Gomez-Heras, M., Benavente, D., Pla, C., Martinez-Martinez, J., Fort, R., & Brotons, V. (2020). Ultrasonic pulse velocity as a way of improving uniaxial compressive strength estimations from Leeb hardness measurements. Construction and Building Materials, 261, 119996. doi:10.1016/j.conbuildmat.2020.119996.

[23] Benavente, D., Martinez-Martinez, J., Galiana-Merino, J. J., Pla, C., de Jongh, M., & Garcia-Martinez, N. (2022). Estimation of uniaxial compressive strength and intrinsic permeability from ultrasounds in sedimentary stones used as heritage building materials. Journal of Cultural Heritage, 55, 346–355. doi:10.1016/j.culher.2022.04.010.

[24] Chen, J., Du, C., Jiang, D., Fan, J., & He, Y. (2016). The mechanical properties of rock salt under cyclic loading-unloading experiments. Geomechanics and Engineering, 10(3), 325–334. doi:10.12989/gae.2016.10.3.325.

[25] Komadja, G. C., Stanislas, T. T., Munganyinka, P., Anye, V., Pradhan, S. P., Adebayo, B., & Onwualu, A. P. (2022).

New approach for assessing uniaxial compressive strength of rocks using measurement from nanoindentation experiments. Bulletin of Engineering Geology and the Environment, 81(8), 299. doi:10.1007/s10064-022-02801-0.

[26] Deere, D. U., & Miller, R. P. (1966). Engineering Classification and Index Properties for Intact Rock. Defense Technical Information Center, Fort Belvoir, United States. doi:10.21236/ad0646610.

[27] Hawkins, A. B., & McConnell, B. J. (1992). Sensitivity of sandstone strength and deformability to changes in moisture content. Quarterly Journal of Engineering Geology, 25(2), 115–130. doi:10.1144/gsl.qjeg.1992.025.02.05.

[28] Lashkaripour, G. R. (2002). Predicting mechanical properties of mudrock from index parameters. Bulletin of Engineering Geology and the Environment, 61(1), 73–77. doi:10.1007/s100640100116.

[29] Yilmaz, I. (2010). Influence of water content on the strength and deformability of gypsum. International Journal of Rock Mechanics and Mining Sciences, 47(2), 342–347. doi:10.1016/j.ijrmms.2009.09.002.

[30] Jaeger, J. C., Cook, N. G., & Zimmerman, R. (2009). Fundamentals of rock mechanics. John Wiley & Sons, Hoboken, United States.

[31] Bieniawski, Z. T. (1974). Estimating the Strength of Rock Materials. Journal of The South African Institute of Mining and Metallurgy, 74(8), 312–320. doi:10.1016/0148-9062(74)91782-3.

[32] Johnston, I. W. (1985). Strength of intact geomechanical materials. Journal of Geotechnical Engineering, 111(6), 730–749. doi:10.1061/(ASCE)0733-9410(1985)111:6(730).

[33] Ramamurthy, T., Rao, G. V., & Rao, K. S. (1985). A strength criterion for rocks. Proceedings of the Indian Geotechnical Conference, 16-18 December, 1985, Roorkee, India.

[34] Hoek, E., & Brown, E. T. (1980). Empirical Strength Criterion for Rock Masses. Journal of the Geotechnical Engineering Division, 106(9), 1013–1035. doi:10.1061/ajgeb6.0001029.

[35] Veríssimo-Anacleto, J., Ludovico-Marques, M., & Neto, P. (2020). An empirical model for compressive strength of the limestone masonry based on number of courses – An experimental study. Construction and Building Materials, 258, 119508. doi:10.1016/j.conbuildmat.2020.119508.

[36] Mahmoodzadeh, A., Mohammadi, M., Hashim Ibrahim, H., Nariman Abdulhamid, S., Ghafoor Salim, S., Farid Hama Ali, H., & Kamal Majeed, M. (2021). Artificial intelligence forecasting models of uniaxial compressive strength. Transportation Geotechnics, 27, 100499. doi:10.1016/j.trgeo.2020.100499.

[37] Alzabeebee, S., Mohammed, D. A., & Alshkane, Y. M. (2022). Experimental Study and Soft Computing Modeling of the Unconfined Compressive Strength of Limestone Rocks Considering Dry and Saturation Conditions. Rock Mechanics and Rock Engineering, 55(9), 5535–5554. doi:10.1007/s00603-022-02948-y.

[38] Lawal, A. I., Kwon, S., Aladejare, A. E., & Oniyide, G. O. (2022). Prediction of the static and dynamic mechanical properties of sedimentary rock using soft computing methods. Geomechanics and Engineering, 28(3), 313–334. doi:10.12989/gae.2022.28.3.313.

[39] Özdemir, E. (2022). A New Predictive Model for Uniaxial Compressive Strength of Rock Using Machine Learning Method: Artificial Intelligence-Based Age-Layered Population Structure Genetic Programming (ALPS-GP). Arabian Journal for Science and Engineering, 47(1), 629–639. doi:10.1007/s13369-021-05761-x.

[40] Jing, L., & Hudson, J. A. (2002). Numerical methods in rock mechanics. International Journal of Rock Mechanics and Mining Sciences, 39(4), 409–427. doi:10.1016/S1365-1609(02)00065-5.

[41] Fuenkajorn, K., & Serata, S. (1993). Numerical simulation of strain-softening and dilation of rock salt. International Journal of Rock Mechanics and Mining Sciences & Geomechanics Abstracts, 30(7), 1303–1306. doi:10.1016/0148-9062(93)90113-r.

[42] Mohammad, N., Reddish, D. J., & Stace, L. R. (1997). The relation between in situ and laboratory rock properties used in numerical modelling. International Journal of Rock Mechanics and Mining Sciences, 34(2), 289–297. doi:10.1016/S0148-9062(96)00060-5.

[43] Lu, Y. B., Li, Q. M., & Ma, G. W. (2010). Numerical investigation of the dynamic compressive strength of rocks based on split Hopkinson pressure bar tests. International Journal of Rock Mechanics and Mining Sciences, 47(5), 829–838. doi:10.1016/j.ijrmms.2010.03.013.

[44] TOKASHIKI, N., & AYDAN, Ö. (2010). the Stability Assessment of Overhanging Ryukyu Limestone Cliffs With an Emphasis on the Evaluation of Tensile Strength of Rock Mass. Doboku Gakkai Ronbunshuu C, 66(2), 397–406. doi:10.2208/jscejc.66.397.

[45] Bidgoli, M. N., Zhao, Z., & Jing, L. (2013). Numerical evaluation of strength and deformability of fractured rocks. Journal of Rock Mechanics and Geotechnical Engineering, 5(6), 419–430. doi:10.1016/j.jrmge.2013.09.002.

[46] Xu, T., Ranjith, P. G., Wasantha, P. L. P., Zhao, J., Tang, C. A., & Zhu, W. C. (2013). Influence of the geometry of partially-spanning joints on mechanical properties of rock in uniaxial compression. Engineering Geology, 167, 134–147. doi:10.1016/j.enggeo.2013.10.011.

[47] Wang, S. Y., Sloan, S. W., Sheng, D. C., Yang, S. Q., & Tang, C. A. (2014). Numerical study of failure behaviour of pre-cracked rock specimens under conventional triaxial compression. International Journal of Solids and Structures, 51(5), 1132–1148. doi:10.1016/j.ijsolstr.2013.12.012.

[48] Rathnaweera, T. D., Ranjith, P. G., Perera, M. S. A., & De Silva, V. R. S. (2017). Development of a laboratory-scale

numerical model to simulate the mechanical behaviour of deep saline reservoir rocks under varying salinity conditions in uniaxial and triaxial test environments. Measurement, 101, 126–137. doi:10.1016/j.measurement.2017.01.015.

[49] Xu, Z. H., Wang, W. Y., Lin, P., Xiong, Y., Liu, Z. Y., & He, S. J. (2020). A parameter calibration method for PFC simulation: Development and a case study of limestone. Geomechanics and Engineering, 22(1), 97–108. doi:10.12989/gae.2020.22.1.097.

[50] Yin, Y., Li, G., Liu, Y., Jiang, X., & Luan, W. (2021). Research on uniaxial compression of jointed rock mass based on numerical simulation. IOP Conference Series: Earth and Environmental Science, 804(2), 22053. doi:10.1088/1755-1315/804/2/022053.

[51] Noorian-Bidgoli, M. (2014). Strength and deformability of fractured rocks. PhD Thesis, KTH Royal Institute of Technology, Stockholm, Sweden.

[52] Itasca, FLAC. (2000). Fast Lagrangian analysis of continua. Itasca Consulting Group Inc., Minneapolis, United States.

[53] Harrison, J. P., & Hudson, J. A. (2000). Introduction. Engineering Rock Mechanics Part II, 3–11, Elsevier, Amsterdam, Netherlands. doi:10.1016/b978-008043010-2/50002-2.

[54] Sano, O., Ito, I., & Terada, M. (1981). Influence of strain rate on dilatancy and strength of Oshima granite under uniaxial compression. Journal of Geophysical Research, 86(B10), 9299–9311. doi:10.1029/JB086iB10p09299.

[55] Mogi, K. (2012). How I developed a true triaxial rock testing machine. True Triaxial Testing of Rocks, 4, 139–157. doi:10.1201/b12705.